Remote Sensing of Environment 315 (2024) 114414

Contents lists available at ScienceDirect

Remote Sensing of Environment

journal homepage: www.elsevier.com/locate/rse

Mobile laser scanning as reference for estimation of stem attributes from airborne laser scanning

Raul de Paula Pires *, Eva Lindberg, Henrik Jan Persson, Kenneth Olofsson, Johan Holmgren

Department of Forest Resource Management, Swedish University of Agricultural Sciences, Umeå, Sweden

ARTICLE INFO

Edited by Marie Weiss

Keywords:
Mobile laser scanning
Forest inventory
Stem diameter
Stem volume
Training data

ABSTRACT

The acquisition of high-quality reference data is essential for effectively modelling forest attributes. Incorporating close-range Light Detection and Ranging (LiDAR) systems into the reference data collection stage of remote sensing-based forest inventories can not only increase data collection efficiency but also increase the number of attributes measured with high quality. Therefore, we propose a model-based forest inventory method that uses reference data collected by a car-mounted mobile laser scanning (MLS) system along boreal forest roads. This approach is used for the estimation of diameter at breast height (DBH) and stem volume at the individual tree-level from airborne laser scanning (ALS) data. In addition, we compare the estimates obtained using the proposed method with the ones derived from reference data collected by traditional field inventory of 265 field plots systematically distributed over the study area. The accuracy of the estimates remained comparable regardless of the reference dataset used for estimation of DBH and stem volume. When using the field inventory dataset for model training, the root mean square error (RMSE) of DBH estimates were 4.06 cm (18.8 %) for Norway spruce trees, 6.3 cm (29.6 %) for Scots pine and 8.61 cm (55.9 %) for deciduous trees. Similarly, when evaluating predictions based on the MLS dataset as reference, RMSEs were equal to 3.97 cm (18.4 %) for Norway spruce, 6.12 cm (28.8 %) for Scots pine, and 8.98 cm (58.3 %) for deciduous trees. In general, biases were below 1 cm for most species classes, with the exception of deciduous trees. The accuracy of stem volume also had RMSEs varying across different tree species. For the estimates based on traditional field inventory, the RMSEs were 0.176 m^3 (38.8 %) for Norway spruce, 0.228 m^3 (52.4 %) for Scots pine and 0.246 m^3 (158 %) for deciduous trees. When using the MLS dataset as a reference, the RMSEs were equal to 0.176 m^3 (38.8 %), 0.228 m^3 (52.4 %), and 0.246 m^3 (158 %) for Norway spruce, Scots pine, and deciduous trees, respectively. Car-mounted MLS demonstrated its potential as an efficient alternative for collecting reference data in remote sensing-based forest inventories, which could complement traditional methods.

1. Introduction

Forests are crucial ecosystems that sustain a diverse range of plant and animal species, while also providing essential services as carbon sequestration, water conservation, and soil stabilization. Moreover, they play a key role in transitioning towards a carbon-neutral economy and mitigating climate change impacts (European Commission, 2021). However, the demand for timber as a renewable material puts pressure on forest resources worldwide, making the establishment of management practices that account for the complexity of forest ecosystems increasingly necessary. Hence, accurate assessments of forest structure and growth are necessary in order to plan interventions that balance the maintenance of biodiversity and sustainable timber production. In response to this need, LiDAR (Light Detection and Ranging) technology is used to obtain auxiliary information in the production of spatially explicit estimations of forest attributes such as growing stock, site index, and biodiversity mapping (Appiah Mensah et al., 2023; Lefsky et al., 2002; Maltamo et al., 2014).

LiDAR-based variables are frequently combined with field reference data to construct predictive models for key forest attributes, such as Diameter at Breast Height (DBH) and stem volume, at individual tree- or area-level (Maltamo et al., 2014). These models are subsequently used to generate wall-to-wall maps of such attributes over large areas, varying from single forest estates to entire countries (Nilsson et al., 2017).

* Corresponding author.
E-mail addresses: raul.de.paula.pires@slu.se (R.P. Pires), eva.lindberg@slu.se (E. Lindberg), henrik.persson@slu.se (H.J. Persson), kenneth.olofsson@slu.se (K. Olofsson), johan.holmgren@slu.se (J. Holmgren).

https://doi.org/10.1016/j.rse.2024.114414
Received 16 May 2024; Received in revised form 16 August 2024; Accepted 5 September 2024
Available online 10 September 2024

In most operational remote sensing-based forest inventories, LiDAR-derived metrics are used to predict forest attributes at area-level, named area-based approach (ABA - Næsset, 2004, Næsset, 2002), with field plot data serving as the reference values in the modelling process (da Bispo et al., 2020; Kotivuori et al., 2016; Leite et al., 2020; Nilsson et al., 2017; Novo-Fernández et al., 2019). Such training data is usually collected using manual methods, which require low start-up cost but can be logistically challenging, since extensive field campaigns are usually necessary in order to sample the complete range of a given forest attribute over large areas (Hyyppä et al., 2020a; Persson et al., 2022; Wang et al., 2016). In addition, the inclusion of variables such as stem profiles and above ground biomass (AGB) in reference data collection can be impractical, requiring destructive techniques or laboratory infrastructure and increase the total cost and time required for sampling (Hauglin et al., 2014; Hunčaga et al., 2020; Stovall et al., 2018). As an alternative, some attributes might not be measured during the surveys but estimated using mathematical models or approximations, which may cause the derived data to be non-representative of the actual forest conditions. For instance, using globally calibrated models on local scale to predict attributes such as AGB can result in biased estimates as demonstrated by Brede et al. (2022) and Calders et al., 2022

Therefore, at the same pace as different LiDAR sensors and platforms become available, authors have explored the suitability of such technologies not only for producing wall-to-wall maps of forest attributes, but also for reference data collection. Different close-range LiDAR sensors such as Terrestrial, Mobile and UAV-borne laser scanners (TLS, MLS and UAVLS, respectively) can collect high-resolution point clouds, proving three-dimensional data with unprecedented level of detail on forest structure and tree architecture (Hyyppä et al., 2020c; Olofsson et al., 2014). With such sensors, it is possible to extract tree attributes such as DBH directly from the point clouds with relatively high accuracy (Brede et al., 2022; Brede et al., 2017; Holmgren et al., 2019; Hyyppä et al., 2020c; Hyyppä et al., 2020b; Kuželka et al., 2020; Olofsson and Holmgren, 2016). For instance, Hyyppä et al. (2020c) found RMSEs of DBH estimates ranging from 2 to 8 % while comparing the performance of different MLSs and UAVLS. In addition, transitioning to LiDAR-based reference data collection could reduce uncertainties related with field measurements (Persson et al., 2022) and enable the sampling of attributes that are difficult to measure by traditional means in large-scale surveys, as stem profiles and branch structure.

Nevertheless, the implementation of LiDAR-based reference data collection in operational scale remains a challenge. Apart from the high acquisition costs, some ground-based LiDAR systems such as TLSs and backpack-mounted or hand-held MLSs have limited scalability, since they are restricted to specific areas or plots, and require labor-intensive surveying campaigns (Calders et al., 2020). Such limitations hinder the operational use, particularly in cases where broad spatial coverage is required. In order to overcome these limitations, researchers have been investigating various combinations of sensors and platforms as potential tools for efficient data collection. As an example, Pires et al. (2022) presented a solution for measuring DBH and stem curves in boreal forests along roads using car-mounted MLS. The study reported DBH measurement accuracies ranging from 1.8 cm to 4.8 cm, which varied depending on the distance of the trees from the roadside. Similarly, Hyyppä et al. (2022) used a high-resolution airborne laser scanning (ALS) system mounted on a helicopter flying at low altitude to measure stem curves and DBH over boreal forest areas, yielding accuracies ranging from 2.2 cm to 2.9 cm in DBH estimation, depending on the test sites. In another study, Hyyppä et al. (2020a) extracted stem curves from below-canopy UAVLS, reaching RMSEs equal to 1.2 cm and 1.4 cm in sparse and obstructed forest plots, respectively (Hyyppä et al., 2020a).

Such combinations of sensors and platforms could enable automatic and detailed forest inventories of large areas and provide researchers and forest managers with a wider range of information, supporting better-informed decision-making. Furthermore, the automation of data collection and analysis can reduce the time and costs associated with traditional field surveys, while also providing more frequent updates on the forest conditions.

Understanding the effect of using innovative data collection methods in large-scale forest inventories is important for ensuring precise and effective forest management. Integrating an additional data collection method, such as car-mounted MLS, into forest inventory could introduce new uncertainties, which depend on the choice of the sensor and platform used for surveying. As an example, the accessibility to certain parts of a forest stand by different platforms, such as all-terrain vehicles, cars, and below-canopy UAVs, may be restricted by terrain and vegetation conditions, resulting in the inability to collect reference data in those areas. Such limitation could result in the systematic inclusion of trees growing under certain condition (e.g. edge effects) in the reference dataset, and these trees might not be representative of the forest as a whole (Delgado et al., 2007; Harper et al., 2015). Moreover, problems with tree detection may lead to certain strata, such as trees with small DBH values, being underrepresented in the reference dataset (Brede et al., 2017; Holmgren et al., 2019; Hyyppä et al., 2020a, 2020b, 2020c; Liu et al., 2021).

With that in mind, this study proposes a model-based forest inventory approach that uses a car-mounted MLS for reference data collection, and compares the estimates obtained using the novel method with those derived from reference data collected by traditional field inventory. With this analysis, we want to contribute to the advancement of remote sensing-based forest inventory methods and elucidate possible implications of using remote sensing-based tools in forest inventory. Specifically, we compare estimates of DBH and stem volume at the individual tree-level by using models trained with different reference datasets. Specific objectives are (i) to train ALS-based models for DBH and stem volume prediction using car-mounted MLS as reference for model training, (ii) to train ALS-based models using field inventory data as reference for model training, and (iii) to compare the estimates generated by both models.

2. Material and methods

2.1. Study area

The study area Remningstorp has approximately 1039 ha (ha) of forest area and is located in Southern Sweden (lat. 58.5 degrees N, long. 13.6 degrees E), in a boreal forest region (Fig. 1). The dominant tree species are Norway spruce (*Picea abies* (L.) H. Karst.) – 85.7 %, Scots pine (*Pinus sylvestris* L.) – 9.1 %, and Birch (*Betula* spp.) – 3.4 %. The average stem density in the area is 580 trees/ha.

2.2. Aerial laser scanning

In October 2019, ALS data was acquired over the study area (Fig. 1) using a Leica Terrain Mapper-LN system mounted on an aircraft. The sensor operated at an altitude of approximately 1450 m and with an average speed of 115 knots, with a pulse frequency of 1600 Hz. The laser beam footprint was 35 cm and the field of view was 30 degrees. The resulting point density in the cloud is 22 points/m^2, on average. Following the acquisition, the ALS point clouds were classified into ground and non-ground using the classification algorithm by Zhang et al. (2016), as implemented in the lidR package (Roussel et al., 2020) in R (R Core Team, 2020).

After the classification, the point cloud was segmented into individual trees using the three-dimensional tree segmentation procedure by Holmgren et al. (2022). In this study, it was assumed that each segment corresponded to one tree crown. Finally, a set of ALS-derived metrics were calculated for each tree segment obtained in the previous step (Table 1). In this study, every 10th height and intensity percentiles, the 95th and 99th height and intensity percentiles, along with descriptive statistics of intensity values, were used as predictors. In addition, a set of tree crown-related attributes, such as crown radius, area, and extent,

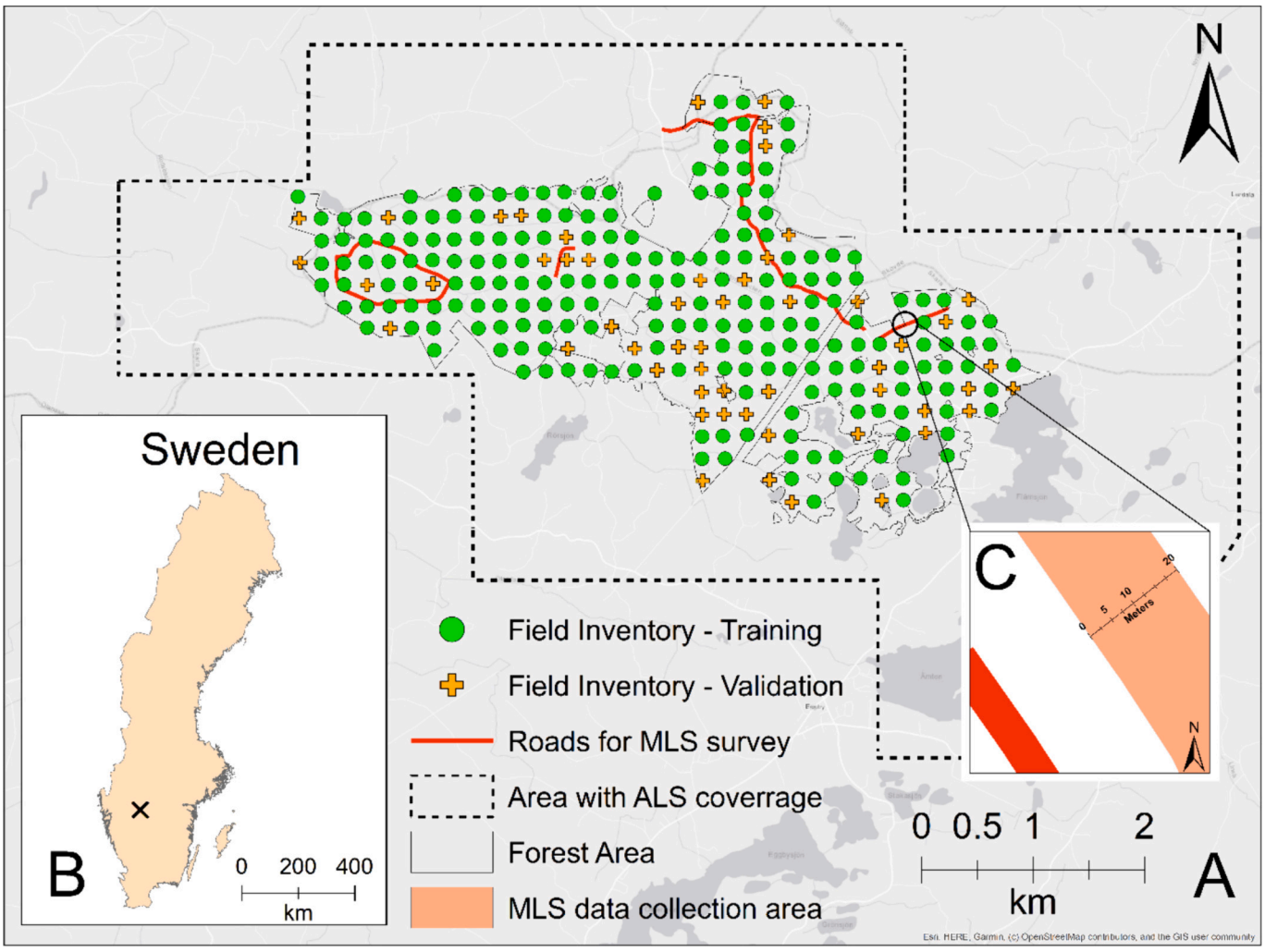

Fig. 1. (A) Overview of the study area, with field plots used for training showed as green circles, the field inventory plots used for validation shown as orange crosses and the roads scanned by the MLS survey in red. (B) Position of the study area in Sweden. (C) Close-up on the area from which MLS data was collected, considering the 20-40 m distance range to the roadside. (For interpretation of the references to colour in this figure legend, the reader is referred to the web version of this article.)

Table 1
Description of the ALS-based metrics used as independent variables in this study.

Metric	Description
$h_{10} - h_{99}$	10th to the 99th height percentiles
$i_{10} - i_{99}$	10th to the 99th intensity percentiles
$mean_i$	Mean of intensity values
std_i	Standard deviation of intensity values
$skew_i$	Skewness of intensity values
kur_i	Kurtosis of intensity values
CR	Crown radius
CA	Crown area
CE	Extent of crown polygon
CRh95	$CR \times h_{95}$
CR^2h95_{sqrt}	$\sqrt{CR^2 \times h_{95}}$

were included in the ALS-based metrics pool for their influence on a tree's DBH (Hemery et al., 2005; Iizuka et al., 2022; Iizuka et al., 2018). These attributes were derived from the delineated tree crown produced by the tree segmentation algorithm. Crown area (CA) was defined as the area of the delineated tree crown and, given that crowns are not perfectly circular, the crown radius (CR) of a tree was defined as the radius of a perfect circle with an area equal to its crown area. Later, the crown extent (CE) was defined as diagonal length of the smallest rectangle containing each crown polygon. Finally, combinations of CR and the 95th height percentile were identified for their significant linear correlation with either DBH or stem volume.

2.3. Reference data collection

We use the terms "reference data" or "training data" to refer to the data used for estimating the model parameters in the model-based inference. In this study, two reference datasets were collected in the study area using different data collection methods. Therefore, we denote the reference dataset obtained through conventional field inventory as the "field inventory dataset", or simply "FI dataset". Similarly, we refer to the reference dataset collected through car-mounted MLS as the "MLS dataset".

2.3.1. Field inventory dataset

The survey using standard field-based forest inventory consisted of a set of 265 circular plots with 10 m radius systematically distributed over the study area (Fig. 1). The plot centers were placed at 200 m distance from each other and, inside each plot, all living trees with DBH $\geq$ 4 cm had the DBH and tree position recorded using a DP POSTEX system (http://www.haglofsweden.com). In each plot, the heights of 1 to 5

sample trees were measured with a hypsometer and the remaining trees had their heights estimated using the model in Eq. (1). The model was adjusted using the ordinary least squares with the height from the sample trees as reference and 95th height percentile from ALS predictor. The model's goodness of fit is shown in the appendix A.

$$\widehat{H} = \beta_0 + \beta_1 \bullet h95 \quad (1)$$

where $\widehat{H}$ is the estimated tree height, $h95$ is the ALS-derived 95th height percentile and β_0 and β_1 are the model parameters. The stem volumes were calculated by using the species-specific volume functions by Brandel (1990).

The tree positions acquired in the field were co-registered with the ones derived from ALS data using the co-registration algorithm by Olofsson et al. (2008). This algorithm aligns the positions of the field-measured trees to the ALS-derived positions using cross-correlation of the position images within a search radius from the field-measured positions. In this step, we used a search radius of 20 m and the ALS-derived positions considered the location of highest point within each ALS-derived tree segment. This step was necessary in order to ensure the correspondence between each field-measured tree and its respective ALS-derived segment. If a segment contained more than one field-recorded tree position, the tree with highest DBH was considered to be the ALS-detected tree (i.e. the one tree represented by the segment) and the other field-recorded trees within that segment were considered omission errors. Segments that did not contain any field-recorded tree positions were considered commission errors.

Altogether, 62 plots had no trees with DBH $\geq$ 4 cm and were not used in this study. Additionally, a visual assessment was conducted in order to assure the quality of the co-registration. The co-registration was considered not successful when the corrected tree positions were outside the plot area or when no field-detected tree was matched to an ALS segment. According to these criteria, the matching procedure was not successful in 9 plots. Finally, 13 plots were overlapping MLS data collection areas and were excluded from the analysis, resulting in 181 plots effectively being used in this study. In terms of individual trees, 3023 field-recorded positions were associated with their respective ALS-derived tree segment in the FI dataset (Fig. 2).

2.3.2. MLS dataset

In 2019, a car-mounted MLS survey was conducted in the study area (Fig. 1). The system consisted of a Riegl VUX1LR laser scanner, synchronized with an Inertial Measurement Unit (IMU) and a GPS/GNSS system, resulting in a georeferenced point cloud with a point registration accuracy of 1.5 cm. The sensor was leaning 30 degrees from the horizontal plane and had 330 degrees of field of view. The car kept an average speed of 8 km/h. Approximately 7 km of forests were scanned along both sides of the road during a 2-h survey. The roads were chosen according to their accessibility by car so the system could measure a large part of the test site without having to turn back. Stem attributes were extracted from the resulting point clouds as described by Pires et al. (2022): first, tree stems were identified in the point clouds using an arc detection procedure. Afterwards, a stem curve model was fitted to each detected tree stem. Finally, DBH and stem volume values were derived from the stem curves of each detected individual.

To ensure the best possible tree detection accuracy and prevent the inclusion of trees influenced by edge effects, Pires et al. (2022) suggested limiting the reference data for model calibration to only include detected trees within the distance range of 20–40 m from the roadside. Considering this range from the roadside and the distance traveled by the car as shown in Fig. 1 - C, the MLS data collection area summed approximately 28 ha of forests, which were used in the study. Moreover, the MLS-derived tree positions showed a systematic displacement in relation to the ALS-derived segments of approximately 1.5 m. Thus, the tree positions were manually adjusted to align the MLS-derived positions with the ALS-detected trees, resulting in 6432 MLS-derived tree positions matching their corresponding ALS-derived tree crowns (Fig. 2).

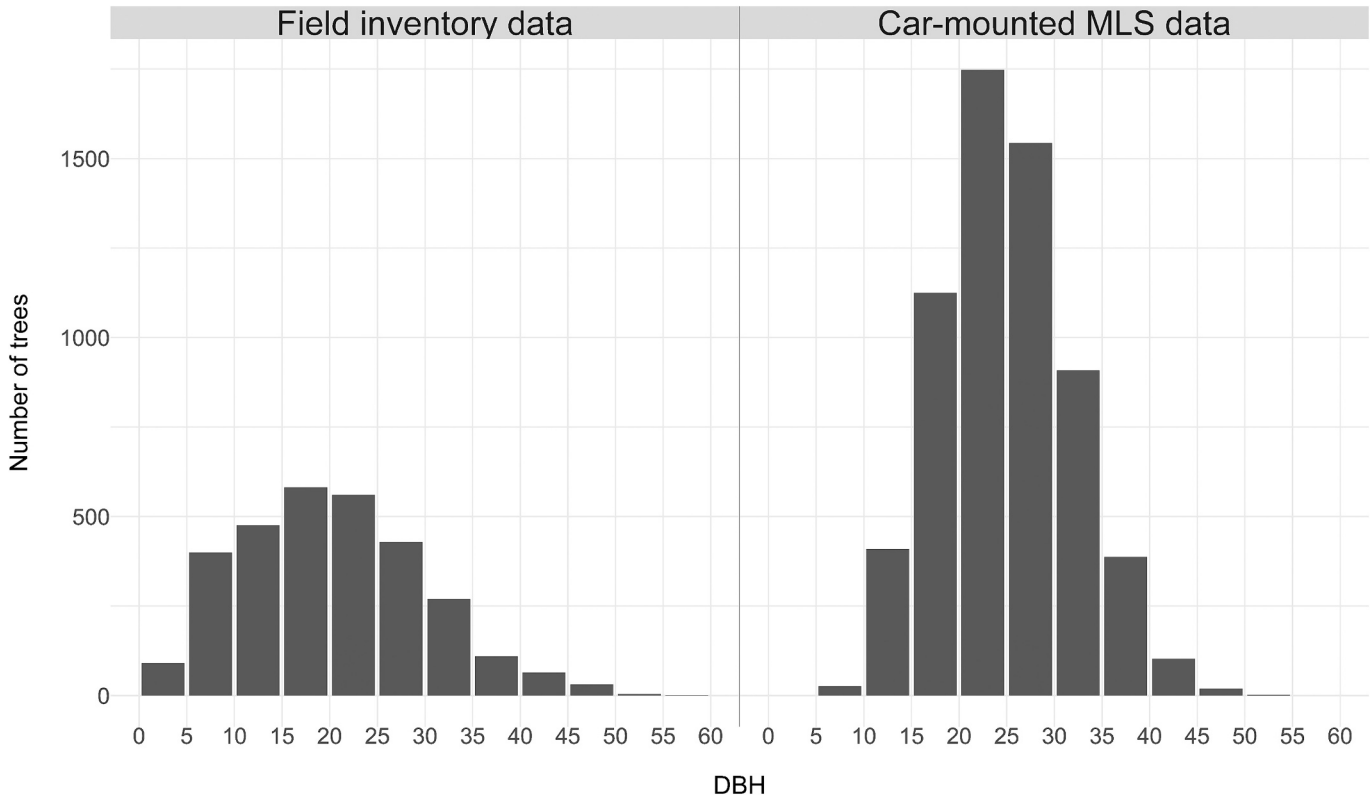

Fig. 2. Diameter at breast height (DBH) distribution of trees associated with an aerial laser scanner-derived tree crown in the Forest inventory and car-mounted mobile laser scanner (MLS) datasets.

2.4. Estimation of forest attributes

Before training the models to estimate stem attributes based on the FI and MLS datasets, the trees in the FI dataset were divided into training and validation groups according to their field plots, creating a benchmark dataset for the MLS- and FI-derived models. Specifically, 70 % of the plots in the FI dataset (2050 trees) were used for model training, while the remaining 30 % (973 trees) were used for validation (Fig. 1 - A). Consequently, the FI-based models were trained on 70 % of the FI dataset, whereas the MLS-based models were trained using the entire MLS dataset. All models were then validated using the validation portion of the FI dataset.

In order to avoid collinearity issues in the models, only the 95th height percentile was considered amongst all height percentiles during variable selection. Ordinary least squares regression was used to estimate the models' coefficients independently for each reference dataset, and the results of the variable selection procedure are presented in the results section. DBH and stem volume estimation models were developed independently for each reference dataset. In this step, the selection of models with different combinations of explanatory variables was carried out using the backwards variable selection method implemented in the caret package (Kuhn, 2020) in R (R Core Team, 2020). Altogether, three models including one to three explanatory variables were evaluated for each reference dataset. The objective was to identify the model that achieved the highest adjusted R^2 value with the fewest number of explanatory variables. To prevent bias in estimating the DBH for trees with small values, the intercept in the DBH prediction model was set to zero. Furthermore, we applied a logarithmic transformation to the stem volume and ALS-derived metrics in order to enhance the linearity in the relationship between explanatory and target variables. To address potential bias introduced by transforming the stem volume before model fitting, we employed the bias correction estimator (b) proposed by Snowdon (1991) - Equation 2). b is estimated separately for each dataset after training the volumetric model (i) and the final volume prediction is calculated by Eq. (3). This approach was adopted to ensure a more accurate and unbiased estimation process.

$$b_i = \sum_{j=1}^{n_i} V_{ij} \Big/ \sum_{j=1}^{n_i} \hat{v}_{ij} \tag{2}$$

$$\hat{V}_{ij} = \hat{v}_{ij} \bullet b_i \tag{3}$$

where n is the number of trees in the dataset i, V_{ij} is the stem volume of tree j from dataset i. $\hat{v}_{ij}$ and $\hat{V}_{ij}$ are the estimated stem volumes of tree j from dataset i before and after bias correction, respectively.

2.5. Accuracy assessment

The accuracy of DBH estimates was assessed by comparing the ALS-derived predictions trained on either the FI or MLS datasets to the field-measured values on the validation portion of the FI dataset at tree-level. Similarly, stem volume estimates were evaluated both at the individual tree- and plot-level by comparing ALS-derived predictions, trained on either the FI or MLS datasets, with the stem volume reference values on the validation subset of the FI dataset. As predictions for both variables were made at the tree level, plot-level estimates of stem volume were obtained by summing up all ALS-derived predictions within the area of each validation plot.

Specifically, the estimates were compared with their respective field-measured values in terms of Root Mean Square Error (RMSE - Eq. (4)) and bias (Eq. (5)). The relative RMSE and bias were calculated in relation to the mean values of the target variables in the FI dataset.

$$RMSE = \sqrt{\sum_{j}^{n} \left(\hat{y}_j - y_j\right)^2 \Big/ n} \tag{4}$$

$$bias = \sum_{j}^{n} \left(\hat{y}_j - y_j\right) \Big/ n \tag{5}$$

where n is the number of trees. $\hat{y}_j$ and y_j are target variable's ALS-derived and field inventory values for tree j.

We used precision (Eq. (6)) and sensitivity (Eq. (7)) to assess the accuracy of the individual tree detection in the validation plots.

$$Precision_p = TP_p \big/ \left(TP_p + C_p\right) \tag{6}$$

$$Sensitivity_p = TP_p \Big/ \left(TP_p + O_p\right) \tag{7}$$

where TP_p is the number of trees correctly detected trees (true positives), $C_p$and O_p are the number of commission and omission errors in plot p.

3. Results

3.1. Individual tree detection

Table 2 shows the mean precision and sensitivity values in different diameter classes. The results indicate that the ITD method used in this study performs best in larger DBH classes, with precision and sensitivity values reaching nearly 100 % in trees greater than 40 cm in DBH. On the other hand, the method had its worst performance in detecting trees with DBHs ranging from 0 to 10 cm, where the highest commission and omission errors were noticed. In general, the performance of ITD in this DBH class negatively affected the overall accuracy of ITD, with approximately 70 % of all omission errors being trees with DBH $\leq$ 10 cm (Fig. 3).

3.2. Modelling forest attributes

Table 4 show the variables selected for different model sizes in the two reference datasets when modelling DBH and stem volume, respectively. In both cases, models with 2 predictors were preferred over other options due to their fewer explanatory variables, despite achieving similar adjusted R^2 values as the other models. Thus, while using the FI dataset, the selected independent variables for the DBH model were h_{95} and CA. Using the MLS dataset, the combination of CRh95 and h_{95} had the best performance in the variable selection step (Table 3). For the stem volume models, h_{95} and CA were chosen as explanatory variables while using either the FI or the MLS dataset for model training (Table 4).

3.3. Prediction of stem attributes

The RMSE of the DBH estimates differed from 0.09 to 0.37 cm when comparing the models trained on the different datasets (Fig. 4). When using the FI dataset as reference, RMSEs ranged from 4.06 cm (18.8 %) in Norway spruce trees to 8.61 cm (55.9 %) in deciduous trees for predictions made a tree-level. When evaluating the predictions made using the MLS dataset as reference, RMSEs ranged from 3.97 cm (18.4 %) in Norway spruce to 8.98 cm (58.3 %) in deciduous trees also at tree-level, as shown in Fig. 4. Most biases were under 1 cm, with exception of the deciduous trees group, which exhibited bias of 2.77 cm (18 %) and 2.32

Table 2
Precision and sensitivity values of Individual Tree Detection (ITD) in Aerial Laser Scanning (ALS) data.

Diameter Class	Precision	Sensitivity
0–10 cm	51.6 %	22.8 %
10–20 cm	71.7 %	66 %
20–30 cm	83 %	89.6 %
30–40 cm	91.5 %	90.9 %
$\geq$ 40 cm	98.5 %	98.5 %
Overall	**81.3 %**	**70.9 %**

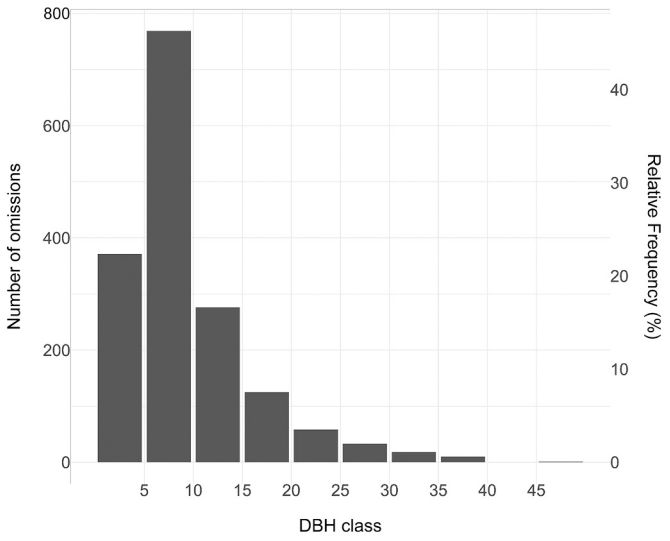

Fig. 3. Histogram of number of omissions and relative frequency in each diameter at breast height (DBH) class. Only trees with DBH ≥ 4 were measured.

Table 3
Models with one, two and three independent variables for DBH (Diameter at Breast Height) estimation using the forest inventory (FI) or car-mounted MLS (MLS). Adj. R^2: adjusted R^2.

N° of predictors	FI dataset		MLS dataset	
	Model	Adj. R^2	Model	Adj. R^2
1	$DBH_{FI} = \alpha_1 \bullet h_{95}$	0.93	$DBH_{MLS} = \alpha_1 \bullet CRh95$	0.96
2	$DBH_{FI} = \alpha_1 \bullet h_{95} + \alpha_2 \bullet CR^2h95_{sqrt}$	0.94	$DBH_{MLS} = \alpha_1 \bullet CRh95 + \alpha_2 \bullet h_{95}$	0.98
3	$DBH_{FI} = \alpha_1 \bullet h_{95} + \alpha_2 \bullet CR^2h95_{sqrt} + \alpha_3 \bullet skew_i$	0.94	$DBH_{MLS} = \alpha_1 \bullet CRh95 + \alpha_2 \bullet h_{95} + \alpha_3 \bullet i_{90}$	0.98

cm (15.1 %) for predictions made using the FI and MLS datasets, respectively.

For stem volume estimates, RMSE values obtained at individual tree-level (Fig. 5) were similar regardless of the dataset used for model training, with RMSEs ranging from 0.176 m^3 (38.8 %) in the Norway spruce group to 0.228 m^3 (52.4 %) in the Scots pine group for the FI-based estimations, as shown in Fig. 5. Meanwhile, the MLS dataset-based estimations per tree species showed RMSEs ranging from 0.176 m^3 (38.8 % - Norway spruce) to 0.246 m^3 (158 % - deciduous). On the other hand, RMSE and bias were lower when comparing the results at plot-level (Fig. 6). In this case, MLS-based predictions had RMSE equal to 46.2 m^3/ha (19.8 %) and bias equal to 2.5 m^3/ha (1.07 %), while FI-based predictions showed RMSE of 43.7 m^3/ha (18.7 %) and bias of −11.5 m^3/ha (−4.92 %), as shown in Fig. 6.

4. Discussion

The purpose of this study was to compare the results from two model-based forest inventory approaches that use on different training datasets. The first training dataset was sampled with traditional field data collection techniques, in other words field plots allocated according to a systematic sampling design and measured using standard equipment such as calipers and hypsometers. In contrast, we assessed the suitability of car-mounted MLS as a method for field data collection. This method uses a purposive sampling design, restricting data collection to a range of 20–40 m from the road network. Overall, both inventory methods resulted in similar models with respect to variable selection and prediction accuracy.

The MLS and FI datasets differed with respect to the sample size and possible measurement errors, which affected the estimated model parameters. With respect to the sample size, while the FI dataset contained 2050 trees for training, the MLS dataset contained 6432 trees. At the same time the training sample size may impact model-based inference (Li et al., 2023), adding reference data does not necessarily enhance estimation accuracy (i.e. RMSE) after a certain threshold (Fassnacht et al., 2014; Lisańczuk et al., 2020). In this context, adequate representation of the modeled trees attribute's variability across the study area may have a more substantial impact on a model's output than the actual size of the training dataset (Junttila et al., 2013). Moreover, both datasets are susceptible to different types of measurement and estimation errors due to limitations from the instruments used during data collection. The DBHs in the FI dataset were measured with calipers, thus being subject to human errors such as challenges associated with measuring at 1.3 m height and incorrect annotation. Additionally, in this dataset the stem volume was estimated by a volumetric model calibrated at landscape-level, potentially introducing bias on the estimates when applied to a local scale as in this study (Brede et al., 2022; Calders et al., 2022).

At the same time, the laser-based measurements of DBH and stem volume on the MLS dataset were subject to different kinds of errors. For instance, Pires et al. (2022) pointed out that the variability in stem detection by the MLS system, influenced by factors such as distance from the sensor to the tree and the presence of branches and understory vegetation around the stem can affect the accuracy of DBH and stem volume values on the MLS dataset. Accurate and precise measurements are crucial when collecting training data as they directly affect the reliability of the resulting models. In this sense, Hyyppä et al. (2022), Hyyppä et al., 2020b, Hyyppä et al., 2020c) suggested that maintaining errors on the training dataset under 10 % would be sufficient to produce accurate models based on close-range laser scanning. Hence, by restricting data collection to a 20–40 m range from the road, we obtained MLS-derived measurements with sufficient quality to produce estimation models with similar prediction accuracy as the ones trained on the FI-dataset. Nevertheless, using data collected closer to the roadside, such as within a 10–20 m range, could potentially improve MLS-based estimates by reducing measurement errors in the MLS dataset. When evaluating the accuracy of estimates in different distance ranges from the roadside, Pires et al. (2022) found that tree detection and estimates of DBH and stem volume within this 10–20 m range had lower errors when compared to estimates from greater distances, such as

Table 4
Models with one, two and three independent variables for stem volume estimation using the forest inventory (FI) or car-mounted MLS (MLS). Adj. R^2: adjusted R^2. $\hat{v}$ is the estimated stem volume before bias correction.

N° of predictors	FI dataset		MLS dataset	
	Model	Adj. R^2	Model	Adj. R^2
1	$\hat{v}_{FI} = e^{\beta_0+\beta_1 \bullet lnh_{95}}$	0.78	$\hat{v}_{MLS} = e^{\beta_0+\beta_1 \bullet lnh_{95}}$	0.74
2	$\hat{v}_{FI} = e^{\beta_0+\beta_1 \bullet lnh_{95}+\beta_2 \bullet lnCA}$	0.80	$\hat{v}_{MLS} = e^{\beta_0+\beta_1 \bullet lnh_{95}+\beta_2 \bullet lnCA}$	0.79
3	$\hat{v}_{FI} = e^{\beta_0+\beta_1 \bullet lnh_{95}+\beta_2 \bullet lnCA+\beta_3 \bullet ln\ h_{10}}$	0.80	$\hat{v}_{MLS} = e^{\beta_0+\beta_1 \bullet lnh_{95}+\beta_2 \bullet lnCA+\beta_3 \bullet lnmean_i}$	0.79

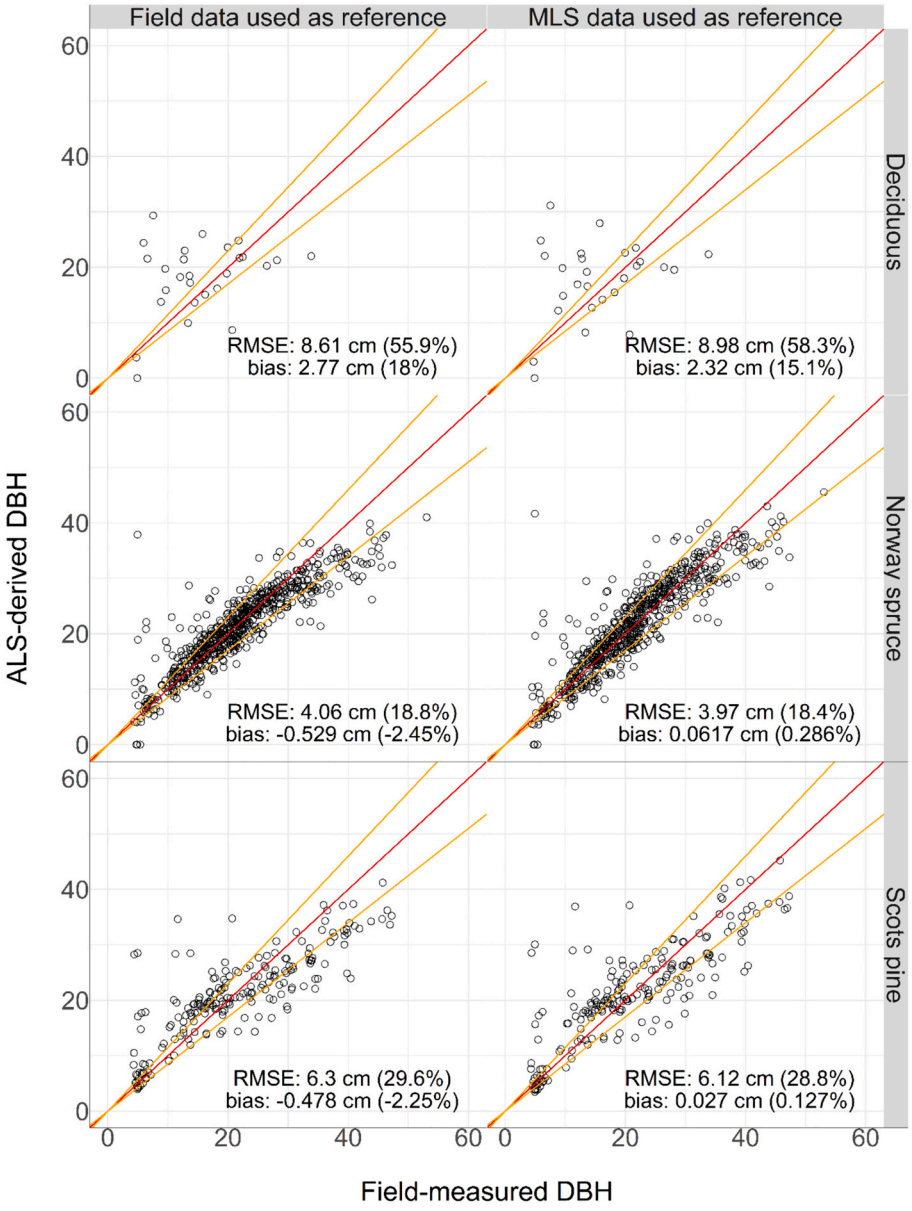

Fig. 4. Field-measured vs. ALS-derived Diameter at Breast Height (DBH), in cm. The columns represent different reference datasets and the rows represent the different species groups. The red line is the 1:1 line, where field-measured and ALS-derived values are equal. The orange lines represent a 15 % deviation from the 1:1 line. RMSE = Root Mean Square Error. (For interpretation of the references to colour in this figure legend, the reader is referred to the web version of this article.)

30–40 m from the roadside. In our analysis, data collected from 0 to 20 m to the roadside was not used for modelling to avoid over-representing trees potentially affected by edge effects in the training data (Harper et al., 2015). However, further analysis is needed to evaluate how including these trees potentially under edge effect in the training data might influence the accuracy and robustness of the prediction models.

Despite the similar model predictions and prediction accuracies evaluated in this study, the DBH errors observed were generally 1–2 cm higher than the ones reported in other studies that aimed at modelling diameter at the individual tree level, when considering the DBH estimation accuracy for the Norway spruce trees. For example, Sun et al. (2022) tested six different modelling methods for DBH prediction at individual tree level of Larch trees (*Larix olgensis* A. Henry), reaching RMSE values ranging from 1.92 cm with artificial neural networks to 2.56 cm with linear regression. However, regardless of the method used, all models tend to underestimate the DBH values of trees with larger diameters. Fu et al. (2020) used a nonlinear mixed-effects model (NLME) for DBH prediction of *Picea crassifolia* (Kom.) trees, reaching RMSE equal to 4.4 cm at individual tree level. Finally, Hao et al. (2021) also used NLME for DBH prediction of Larch trees, yield RMSE of 1.94 cm at individual tree level with the inclusion of site-specific random effects, which significantly improved the model's performance.

The errors in DBH estimation noticed in our study could have been caused different factors, such as the complexity of the target variable being modeled and the robustness of the statistical models used for prediction, which may involve considerations regarding model assumptions, parameter estimation methods, and the incorporation of relevant covariates or predictors. In addition, the different accuracies in the estimation of DBH and stem volume across species groups can be partially explained by the fact that Norway spruce is the main tree species in the study area, accounting for 85.7 % of all trees, which caused the models to be optimized for this specific species. For this target variable, the inclusion of site- and species-specific relationships between DBH and the explanatory variables could potentially improve the accuracy of our predictions (Hao et al., 2021; Raumonen et al., 2015).

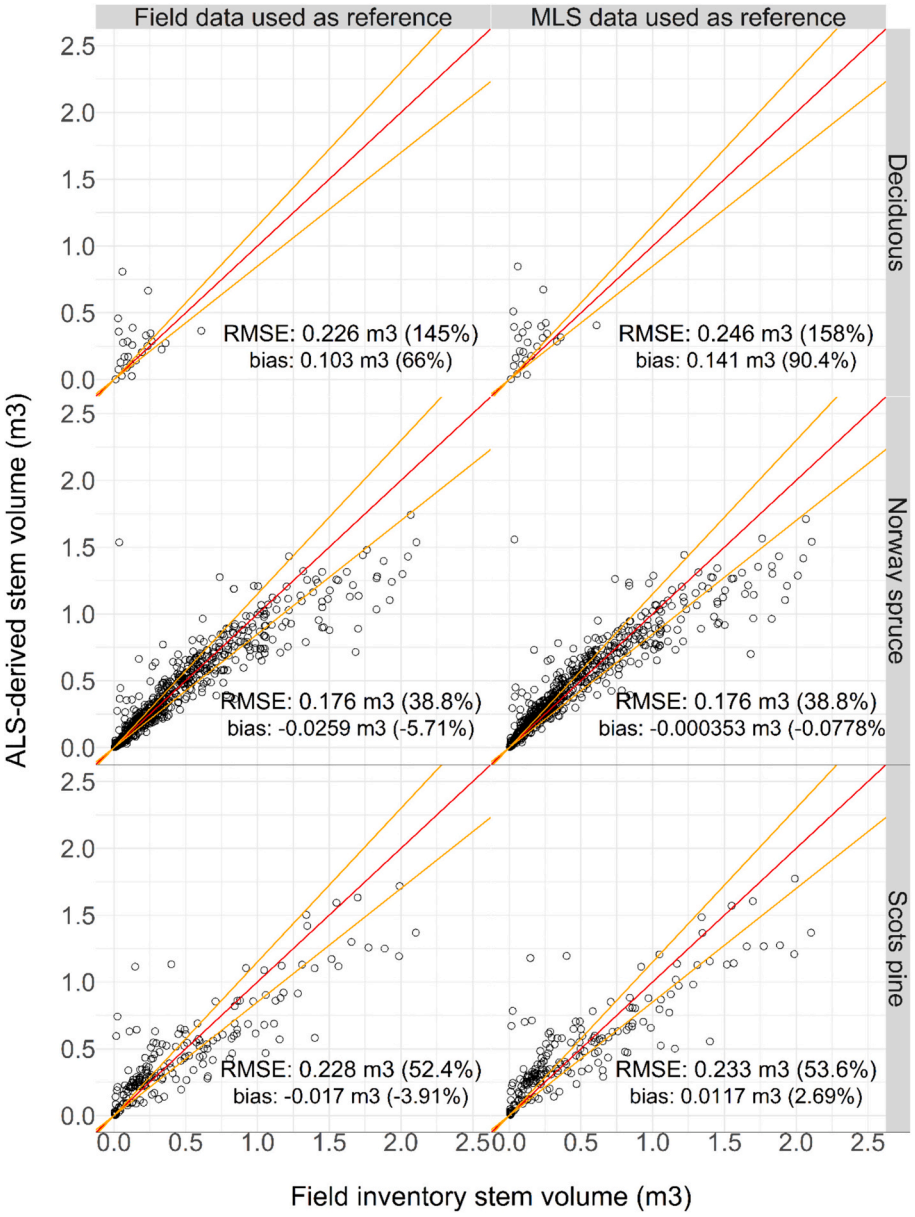

Fig. 5. Individual tree-level field inventory vs. ALS-derived stem volume, in m^3. The columns represent different reference datasets and the rows represent the different species groups. The red line is the 1:1 line, where the field inventory and ALS-derived values are equal. The orange lines represent a 15 % deviation from the 1:1 line. RMSE = Root Mean Square Error. (For interpretation of the references to colour in this figure legend, the reader is referred to the web version of this article.)

Analogously, individual tree-level estimates of stem volume may also be improved by using different modelling techniques, such as generalized linear models and non-parametric estimation methods (Hauglin et al., 2018). For instance, Karjalainen et al. (2019) reached generally lower relative RMSEs for this variable, which varied from 29 % to 41 %, while testing the transferability of a non-parametric stem volume model amongst different sites. When aggregated to plot-level (Fig. 5), the values obtained in this study were in-line with other volume estimation methods, which reported RMSEs ranging from 15.5 % to 56.2 % in boreal and temperate forest conditions (Kandare et al., 2017; Kankare et al., 2011; Kukkonen et al., 2021; Vastaranta et al., 2012; Yu et al., 2010). Similarly, Puliti et al. (2020) observed decreasing errors when comparing volume estimates at coarser levels, reaching relative RMSEs of 32.2 %, 27.1 % and 3.5 % at plot-, stand- and forest-level, respectively, while assessing the potential of UAVLS in estimating growing stock without field data for model calibration. Furthermore, Hauglin et al. (2018) used accurately positioned harvester data as reference for volume models and reported relative RMSEs ranging from 19 % to 60 % at plot-level, depending on the forest strata.

Omission and commission errors in individual tree detection can also influence the accuracy of plot-level volume estimates. In this study, omission errors were also the most pronounced in small DBH classes, resulting in sensitivities equal to 22.8 % in trees from 0 to 10 cm and 66 % in trees from 10 to 20 cm. Although these classes account for a smaller proportion of the total volume, cumulative omissions can result in significant bias in total or mean values. This kind of detection error is a common cause of stem volume underestimation when aggregating tree-level results to an area unit (Kandare et al., 2017; Kukkonen et al., 2021; Sačkov et al., 2019; Vastaranta et al., 2012), as the omission of trees in the suppressed or understory forest layers is common in ITD algorithms. For instance, Wang et al. (2016) found omission rates varying from approximately 40 % to nearly 100 % of suppressed trees when comparing 9 distinct ITD algorithms in boreal forest conditions. Analogously, Sparks et al. (2022) reported higher rates of omissions in

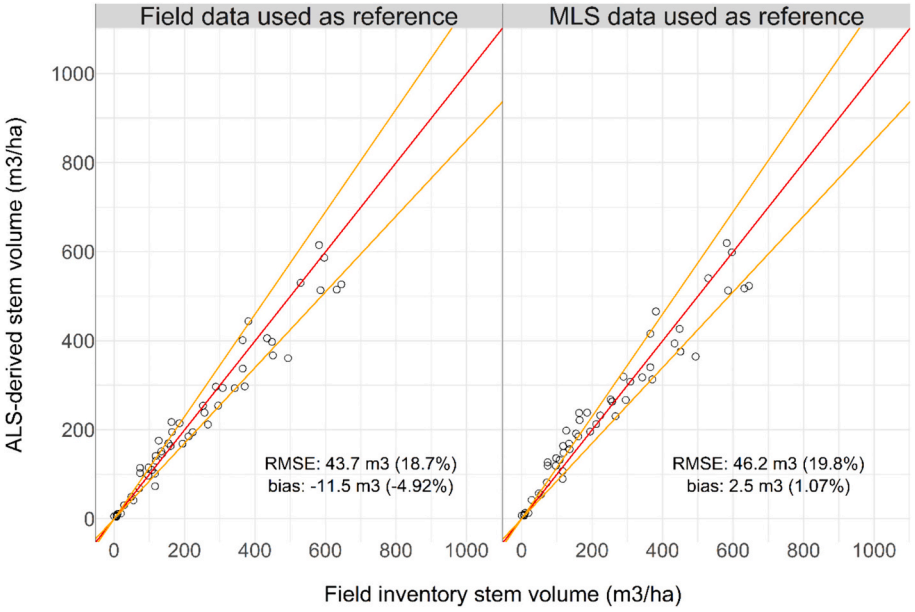

Fig. 6. Plot-level field inventory vs. ALS-derived stem volume, in m^3. The columns represent different reference datasets. The red line is the 1:1 line, where the field inventory and ALS-derived values are equal. The orange lines represent a 15 % deviation from the 1:1 line. RMSE = Root Mean Square Error. (For interpretation of the references to colour in this figure legend, the reader is referred to the web version of this article.)

suppressed trees when benchmarking ITD algorithms in mixed-conifer temperate forests.

Finally, future studies should focus on improving individual tree-level DBH and stem volume models, as well as exploring the estimation of tree species using remote sensing data. Potential improvements in tree attribute estimation and accurate identification of tree species would significantly contribute to more accurate and ecologically informed forest inventory and management practices.

5. Conclusion

In our analysis, we found that the estimation models trained with either the FI or MLS datasets presented similar values for RMSE and bias for estimates of DBH and stem volume at individual tree level. This implies that both methods perform similarly and hence the use of MLS for training data collection instead of conventional field inventory can save time and costs. Nevertheless, the results obtained in this study are limited to a Norway spruce dominated boreal forest ecosystem. Therefore, future analyses, such as the proposed method's performance in different forest conditions and the impact of seasonal environment variations on the data quality, are needed to fully elucidate the capabilities and limitations of car-mounted MLS for training data collection.

CRediT authorship contribution statement

Raul de Paula Pires: Writing – review & editing, Writing – original draft, Visualization, Validation, Methodology, Formal analysis, Conceptualization. **Eva Lindberg:** Writing – review & editing, Supervision, Resources, Methodology, Conceptualization. **Henrik Jan Persson:** Writing – review & editing, Supervision, Methodology, Conceptualization. **Kenneth Olofsson:** Writing – review & editing, Supervision, Methodology, Conceptualization. **Johan Holmgren:** Writing – review & editing, Supervision, Software, Resources, Methodology, Funding acquisition, Conceptualization.

Declaration of competing interest

The authors declare the following financial interests/personal relationships which may be considered as potential competing interests.

Raul de Paula Pires reports financial support was provided by Stora Enso AB.

Data availability

The authors do not have permission to share data.

Acknowledgements

This study was financed by Stora Enso, and the Kempe foundations through the project "Estimating Forest Resources and Quality-related Attributes Using Automated Methods and Technologies" which was part of the Tandem Forest values research program (Grant Number TF 2019-0064). In addition, funding was provided by the Hildur and Sven Wingquist foundation for forest science research though the project "Multi sensor remote sensing for improved information in forest management planning" (Grant number 17/18-2 / 107-5 SOJOH) and the Bo Rydin Foundation for Scientific Research thought the project "F 06/21 Multi-phase inventory of forest using high-resolution laser scanning". Finally, co-financing was provided by the Swedish Foundation for Strategic Environmental Research with the research program Mistra Digital Forest (DIA 2017/14 #6).

Appendix A. Appendix

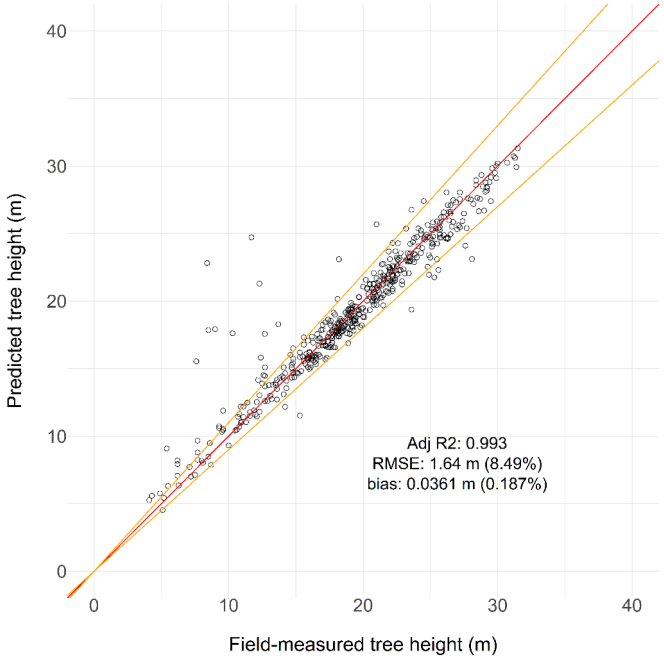

Fig 1. A – Goodness of fit of tree height estimation model based on the 95th height percentile from aerial laser scanning data

References

Appiah Mensah, A., Jonzén, J., Nyström, K., Wallerman, J., Nilsson, M., 2023. Mapping site index in coniferous forests using bi-temporal airborne laser scanning data and field data from the Swedish national forest inventory. For. Ecol. Manag. 547 https://doi.org/10.1016/j.foreco.2023.121395.

Brandel, G., 1990. Volymfunktioner för Enskilda Träd : Tall, Gran Och björk = Volume Functions for Individual Trees : Scots Pine (*Pinus sylvestris*), Norway Spruce (*Picea abies*) and Birch (Betula Pendula & *Betula pubescens*). Swedish Univ. Agric. Sci. Skogsfakta 11, 1-10. Garpenberg.

Brede, B., Lau, A., Bartholomeus, H.M., Kooistra, L., 2017. Comparing RIEGL RiCOPTER UAV LiDAR derived canopy height and DBH with terrestrial LiDAR. Sensors (Switzerland) 17, 1–16. https://doi.org/10.3390/s17102371.

Brede, B., Terryn, L., Barbier, N., Bartholomeus, H.M., Bartolo, R., Calders, K., Derroire, G., Krishna Moorthy, S.M., Lau, A., Levick, S.R., Raumonen, P., Verbeeck, H., Wang, D., Whiteside, T., van der Zee, J., Herold, M., 2022. Non-destructive estimation of individual tree biomass: Allometric models, terrestrial and UAV laser scanning. Remote Sens. Environ. 280 https://doi.org/10.1016/j.rse.2022.113180.

Calders, K., Adams, J., Armston, J., Bartholomeus, H., Bauwens, S., Bentley, L.P., Chave, J., Danson, F.M., Demol, M., Disney, M., Gaulton, R., Krishna Moorthy, S.M., Levick, S.R., Saarinen, N., Schaaf, C., Stovall, A., Terryn, L., Wilkes, P., Verbeeck, H., 2020. Terrestrial laser scanning in forest ecology: expanding the horizon. Remote Sens. Environ. 251, 112102 https://doi.org/10.1016/j.rse.2020.112102.

Calders, K., Verbeeck, H., Burt, A., Origo, N., Nightingale, J., Malhi, Y., Wilkes, P., Raumonen, P., Bunce, R.G.H., Disney, M., 2022. Laser scanning reveals potential underestimation of biomass carbon in temperate forest. Ecol. Solut. Evid. 3, 1–14. https://doi.org/10.1002/2688-8319.12197.

da Bispo, P.C., Rodríguez-Veiga, P., Zimbres, B., de Miranda, S.C., do Cezare, C.H.G., Fleming, S., Baldacchino, F., Louis, V., Rains, D., Garcia, M., Espírito-Santo, F.D.B., Roitman, I., Pacheco-Pascagaza, A.M., Gou, Y., Roberts, J., Barrett, K., Ferreira, L.G., Shimbo, J.Z., Alencar, A., Bustamante, M., Woodhouse, I.H., Sano, E.E., Ometto, J.P., Tansey, K., Balzter, H., 2020. Woody aboveground biomass mapping of the brazilian savanna with a multi-sensor and machine learning approach. Remote Sens. 12 https://doi.org/10.3390/RS12172685.

Delgado, J.D., Arroyo, N.L., Arévalo, J.R., Fernández-Palacios, J.M., 2007. Edge effects of roads on temperature, light, canopy cover, and canopy height in laurel and pine forests (Tenerife, Canary Islands). Landsc. Urban Plan. 81, 328–340. https://doi.org/10.1016/j.landurbplan.2007.01.005.

European Commission, 2021. New EU Forest Strategy for 2030, Communication from the Commission to the European Parliment, the Council, the European Economic and Social Committee of the regions. https://doi.org/10.2307/j.ctv2zp4wq1.5.

Fassnacht, F.E., Hartig, F., Latifi, H., Berger, C., Hernández, J., Corvalán, P., Koch, B., 2014. Importance of sample size, data type and prediction method for remote sensing-based estimations of aboveground forest biomass. Remote Sens. Environ. 154, 102–114. https://doi.org/10.1016/j.rse.2014.07.028.

Fu, L., Duan, G., Ye, Q., Meng, X., Luo, P., Sharma, R.P., Sun, H., Wang, G., Liu, Q., 2020. Prediction of individual tree diameter using a nonlinear mixed-effects modeling approach and airborne LiDAR data. Remote Sens. 12 https://doi.org/10.3390/rs12071066.

Hao, Y., Widagdo, F.R.A., Liu, X., Quan, Y., Dong, L., Li, F., 2021. Individual tree diameter estimation in small-scale forest inventory using uav laser scanning. Remote Sens. 13, 1–21. https://doi.org/10.3390/rs13010024.

Harper, K.A., Macdonald, S.E., Mayerhofer, M.S., Biswas, S.R., Esseen, P.A., Hylander, K., Stewart, K.J., Mallik, A.U., Drapeau, P., Jonsson, B.G., Lesieur, D., Kouki, J., Bergeron, Y., 2015. Edge influence on vegetation at natural and anthropogenic edges of boreal forests in Canada and Fennoscandia. J. Ecol. 103, 550–562. https://doi.org/10.1111/1365-2745.12398.

Hauglin, M., Gobakken, T., Astrup, R., Ene, L., Næsset, E., 2014. Estimating single-tree crown biomass of Norway spruce by airborne laser scanning: a comparison of methods with and without the use of terrestrial laser scanning to obtain the ground reference data. Forests 5, 384–403. https://doi.org/10.3390/f5030384.

Hauglin, M., Hansen, E., Sørngård, E., Næsset, E., Gobakken, T., 2018. Utilizing accurately positioned harvester data: modelling forest volume with airborne laser scanning. Can. J. For. Res. 48, 913–922. https://doi.org/10.1139/cjfr-2017-0467.

Hemery, G.E., Savill, P.S., Pryor, S.N., 2005. Applications of the crown diameter-stem diameter relationship for different species of broadleaved trees. For. Ecol. Manag. 215, 285–294. https://doi.org/10.1016/j.foreco.2005.05.016.

Holmgren, J., Tulldahl, M., Nordlöf, J., Willén, E., Olsson, H., 2019. Mobile laser scanning for estimating tree stem diameter using segmentation and tree spine calibration. Remote Sens. 11, 1–18. https://doi.org/10.3390/rs11232781.

Holmgren, J., Lindberg, E., Olofsson, K., Persson, H.J., 2022. Tree crown segmentation in three dimensions using density models derived from airborne laser scanning. Int. J. Remote Sens. 43, 299–329. https://doi.org/10.1080/01431161.2021.2018149.

Hunčaga, M., Chudá, J., Tomaštík, J., Slámová, M., Koreň, M., Chudý, F., 2020. The comparison of stem curve accuracy determined from point clouds acquired by different terrestrial remote sensing methods. Remote Sens. 12 https://doi.org/10.3390/RS12172739.

Hyyppä, E., Hyyppä, J., Hakala, T., Kukko, A., Wulder, M.A., White, J.C., Pyörälä, J., Yu, X., Wang, Y., Virtanen, J.P., Pohjavirta, O., Liang, X., Holopainen, M., Kaartinen, H., 2020a. Under-canopy UAV laser scanning for accurate forest field measurements. ISPRS J. Photogramm. Remote Sens. 164, 41–60. https://doi.org/10.1016/j.isprsjprs.2020.03.021.

Hyyppä, E., Kukko, A., Kaijaluoto, R., White, J.C., Wulder, M.A., Pyörälä, J., Liang, X., Yu, X., Wang, Y., Kaartinen, H., Virtanen, J.P., Hyyppä, J., 2020b. Accurate derivation of stem curve and volume using backpack mobile laser scanning. ISPRS J. Photogramm. Remote Sens. 161, 246–262. https://doi.org/10.1016/j.isprsjprs.2020.01.018.

Hyyppä, E., Yu, X., Kaartinen, H., Hakala, T., Kukko, A., Vastaranta, M., Hyyppä, J., 2020c. Comparison of backpack, handheld, under-canopy UAV, and above-canopy

UAV laser scanning for field reference data collection in boreal forests. Remote Sens. 12, 1–31. https://doi.org/10.3390/rs12203327.
Hyyppä, E., Kukko, A., Kaartinen, H., Yu, X., Muhojoki, J., Hakala, T., Hyyppä, J., 2022. Direct and automatic measurements of stem curve and volume using a high-resolution airborne laser scanning system. Sci. Remote Sens. 5, 100050 https://doi.org/10.1016/j.srs.2022.100050.
Iizuka, K., Yonehara, T., Itoh, M., Kosugi, Y., 2018. Estimating tree height and diameter at breast height (DBH) from digital surface models and orthophotos obtained with an unmanned aerial system for a Japanese cypress (Chamaecyparis obtusa) Forest. Remote Sens. 10 https://doi.org/10.3390/rs10010013.
Iizuka, K., Kosugi, Y., Noguchi, S., Iwagami, S., 2022. Toward a comprehensive model for estimating diameter at breast height of Japanese cypress (Chamaecyparis obtusa) using crown size derived from unmanned aerial systems. Comput. Electron. Agric. 192, 106579 https://doi.org/10.1016/j.compag.2021.106579.
Junttila, V., Finley, A.O., Bradford, J.B., Kauranne, T., 2013. Strategies for minimizing sample size for use in airborne LiDAR-based forest inventory. For. Ecol. Manag. 292, 75–85. https://doi.org/10.1016/j.foreco.2012.12.019.
Kandare, K., Dalponte, M., Ørka, H.O., Frizzera, L., Næsset, E., 2017. Prediction of species-specific volume using different inventory approaches by fusing airborne laser scanning and hyperspectral data. Remote Sens. 9, 1–19. https://doi.org/10.3390/rs9050400.
Kankare, V., Vastaranta, M., Holopainen, M., Yu, X., Hyyppä, J., Hyyppä, H., 2011. The fusion of individual tree detection and visual interpretation in assessment of Forest variables from laser point clouds. Int. Arch. Photogramm. Remote. Sens. Spat. Inf. Sci. 157–161. https://doi.org/10.5194/isprsarchives-xxxviii-5-w12-157-2011. XXXVIII-5/.
Karjalainen, T., Korhonen, L., Packalen, P., Maltamo, M., 2019. The transferability of airborne laser scanning based tree-level models between different inventory areas. Can. J. For. Res. 49, 228–236. https://doi.org/10.1139/cjfr-2018-0128.
Kotivuori, E., Korhonen, L., Packalen, P., 2016. Nationwide airborne laser scanning based models for volume, biomass and dominant height in Finland. Silva Fenn. 50, 1–28. https://doi.org/10.14214/sf.1567.
Kuhn, M., 2020. Caret: Classification and Regression Training. R Package Version 6.0–86. https://CRAN.R-project.org/package=caret.
Kukkonen, M., Maltamo, M., Korhonen, L., Packalen, P., 2021. Fusion of crown and trunk detections from airborne UAS based laser scanning for small area forest inventories. Int. J. Appl. Earth Obs. Geoinf. 100, 102327 https://doi.org/10.1016/j.jag.2021.102327.
Kuželka, K., Slavík, M., Surový, P., 2020. Very high density point clouds from UAV laser scanning for automatic tree stem detection and direct diameter measurement. Remote Sens. 12 https://doi.org/10.3390/RS12081236.
Lefsky, M.A., Cohen, W.B., Parker, G.G., Harding, D.J., 2002. Lidar Remote Sensing for Ecosystem Studies, 52, 19–30.
Leite, R.V., Silva, C.A., Mohan, M., Cardil, A., de Almeida, D.R.A., de e Carvalho, S.P.C., Jaafar, W.S.W.M., Hernández, J.G., Weiskittel, A., Hudak, A.T., Broadbent, E.N., Prata, G., Valbuena, R., Leite, H.G., Taquetti, M.F., Soares, A.A.V., Scolforo, H.F., Do Amaral, C.H., Corte, A.P.D., Klauberg, C., 2020. Individual tree attribute estimation and uniformity assessment in fast-growing eucalyptus spp. Forest plantations using lidar and linear mixed-effects models. Remote Sens. 12, 1–20. https://doi.org/10.3390/rs12213599.
Li, C., Yu, Z., Dai, H., Zhou, X., Zhou, M., 2023. Effect of sample size on the estimation of forest inventory attributes using airborne LiDAR data in large-scale subtropical areas. Ann. For. Sci. 80 https://doi.org/10.1186/s13595-023-01209-4.
Lisańczuk, M., Mitelsztedt, K., Parkitna, K., Krok, G., Stereńczak, K., Wysocka-Fijorek, E., Miścicki, S., 2020. Influence of sampling intensity on performance of two-phase forest inventory using airborne laser scanning. For. Ecosyst. 7 https://doi.org/10.1186/s40663-020-00277-6.
Liu, L., Zhang, A., Xiao, S., Hu, S., He, N., Pang, H., Zhang, X., Yang, S., 2021. Single tree segmentation and diameter at breast height estimation with mobile LiDAR. IEEE Access 9, 24314–24325. https://doi.org/10.1109/ACCESS.2021.3056877.
Maltamo, M., Næsset, E., Vauhkonen, J., 2014. Forestry applications of airborne laser scanning: concepts and case studies, Springer Netherlands, Dordrecht. https://doi.org/10.1007/978-94-017-8663-8.
Næsset, E., 2002. Predicting forest stand characteristics with airborne scanning laser using a practical two-stage procedure and field data. Remote Sens. Environ. 80, 88–99. https://doi.org/10.1016/S0034-4257(01)00290-5.
Næsset, E., 2004. Practical large-scale forest stand inventory using a small-footprint airborne scanning laser. Scand. J. For. Res. 19, 164–179. https://doi.org/10.1080/02827580310019257.
Nilsson, M., Nordkvist, K., Jonzén, J., Lindgren, N., Axensten, P., Wallerman, J., Egberth, M., Larsson, S., Nilsson, L., Eriksson, J., Olsson, H., 2017. A nationwide forest attribute map of Sweden predicted using airborne laser scanning data and field data from the national forest inventory. Remote Sens. Environ. 194, 447–454. https://doi.org/10.1016/j.rse.2016.10.022.
Novo-Fernández, A., Barrio-Anta, M., Recondo, C., Cámara-Obregón, A., López-Sánchez, C.A., 2019. Integration of national forest inventory and nationwide airborne laser scanning data to improve forest yield predictions in North-Western Spain. Remote Sens. 11, 1–25. https://doi.org/10.3390/rs11141693.
Olofsson, K., Holmgren, J., 2016. Single tree stem profile detection using terrestrial laser scanner data, flatness saliency features and curvature properties. Forests 7, 207. https://doi.org/10.3390/f7090207.
Olofsson, K., Lindberg, E., Holmgren, J., 2008. A method for linking field-surveyed and aerial-detected single trees using cross correlation of position images and the optimization of weighted tree list graphs. Hill RA, rosette J, Suárez J proc. SilviLaser 2008. In: 8th Int. Conf. LiDAR Appl. For. Assess. Invent. Heriot-Watt Univ. Edinburgh, UK, 17–19 Sept. 2008, pp. 95–104.
Olofsson, K., Holmgren, J., Olsson, H., 2014. Tree stem and height measurements using terrestrial laser scanning and the RANSAC algorithm. Remote Sens. 6, 4323–4344. https://doi.org/10.3390/rs6054323.
Persson, H.J., Olofsson, K., Holmgren, J., 2022. Two-phase forest inventory using very-high-resolution laser scanning. Remote Sens. Environ. 271, 112909 https://doi.org/10.1016/j.rse.2022.112909.
Pires, R. de P., Olofsson, K., Persson, H.J., Lindberg, E., Holmgren, J., 2022. Individual tree detection and estimation of stem attributes with mobile laser scanning along boreal forest roads. ISPRS J. Photogramm. Remote Sens. 187, 211–224. https://doi.org/10.1016/j.isprsjprs.2022.03.004.
Puliti, S., Breidenbach, J., Astrup, R., 2020. Estimation of forest growing stock volume with UAV laser scanning data: can it be done without field data? Remote Sens. 12, 1245. https://doi.org/10.3390/RS12081245.
R Core Team, 2020. R: A Language and Environment for Statistical Computing. R Foundation for Statistical Computing.
Raumonen, P., Casella, E., Calders, K., 2015. Massive-Scale Tree Modelling from TLS Data. https://doi.org/10.5194/isprsannals-II-3-W4-189-2015.
Roussel, J.R., Auty, D., Coops, N.C., Tompalski, P., Goodbody, T.R.H., Meador, A.S., Bourdon, J.F., de Boissieu, F., Achim, A., 2020. lidR: an R package for analysis of airborne laser scanning (ALS) data. Remote Sens. Environ. 251, 112061 https://doi.org/10.1016/j.rse.2020.112061.
Sačkov, I., Scheer, A., Bucha, T., 2019. A comparison of two tree detection methods for estimation of Forest stand and ecological variables from airborne LiDAR data in central European forests. Cent. Eur. For. J. 11 https://doi.org/10.3390/rs11121431.
Snowdon, P., 1991. A ratio estimator for bias correction in logarithmic regressions. Can. J. For. Res. 21, 720–724.
Sparks, A.M., Corrao, M.V., Smith, A.M.S., 2022. Cross-comparison of individual tree detection methods using low and high pulse density airborne laser scanning data. Remote Sens. 14 https://doi.org/10.3390/rs14143480.
Stovall, A.E.L., Anderson-teixeira, K.J., Shugart, H.H., 2018. Assessing terrestrial laser scanning for developing non-destructive biomass allometry. For. Ecol. Manag. 427, 217–229. https://doi.org/10.1016/j.foreco.2018.06.004.
Sun, Y., Jin, X., Pukkala, T., Li, F., 2022. Predicting individual tree diameter of larch (Larix olgensis) from UAV-LiDAR data using six different algorithms. Remote Sens. 14 https://doi.org/10.3390/rs14051125.
Vastaranta, M., Kankare, V., Holopainen, M., Yu, X., Hyyppä, J., Hyyppä, H., 2012. Combination of individual tree detection and area-based approach in imputation of forest variables using airborne laser data. ISPRS J. Photogramm. Remote Sens. 67, 73–79. https://doi.org/10.1016/j.isprsjprs.2011.10.006.
Wang, Y., Hyyppa, J., Liang, X., Kaartinen, H., Yu, X., Lindberg, E., Holmgren, J., Qin, Y., Mallet, C., Ferraz, A., Torabzadeh, H., Morsdorf, F., Zhu, L., Liu, J., Alho, P., 2016. International benchmarking of the individual tree detection methods for modeling 3-D canopy structure for Silviculture and Forest ecology using airborne laser scanning. IEEE Trans. Geosci. Remote Sens. 54, 5011–5027. https://doi.org/10.1109/TGRS.2016.2543225.
Yu, X., Hyyppä, J., Holopainen, M., Vastaranta, M., 2010. Comparison of area-based and individual tree-based methods for predicting plot-level forest attributes. Remote Sens. 2, 1481–1495. https://doi.org/10.3390/rs2061481.
Zhang, W., Qi, J., Wan, P., Wang, H., Xie, D., Wang, X., Yan, G., 2016. An easy-to-use airborne LiDAR data filtering method based on cloth simulation. Remote Sens. 8, 1–22. https://doi.org/10.3390/rs8060501.